Two-Step Formation of Streptavidin-Supported Lipid Bilayers by PEG-Triggered Vesicle Fusion. Fluorescence and Atomic Force Microscopy Characterization†

Alexandre Berquand,§ Pierre-Emmanuel Mazeran,§ Jacques Pantigny,‡ Vanessa Proux-Delrouyre,‡ Jean-Marc Laval,‡ and Christian Bourdillon*,‡

Laboratoire de Technologie Enzymatique, CNRS UMR 6022, and Laboratoire Roberval, Unité de Recherche en Mécanique, CNRS UMR 6066, Université de Technologie de Compiègne, B. P. 20529, 60205 Compiègne Cedex, France

Received May 31, 2002. In Final Form: August 29, 2002

We have used fluorescence microscopy, fluorescence photobleaching recovery (FPR), and atomic force microscopy (AFM) to investigate the formation of tethered lipid bilayers on plane aluminum oxide or glass surfaces. The bilayers were assembled with the help of a two-step methodology recently proposed for microporous templates (Proux-Delrouyre et al. *J. Am. Chem. Soc.* **2001**, *123*, 8313). The first step consists of the accumulation of intact biotinylated vesicles (PC + DOPE) on a streptavidin sublayer itself immobilized on the substrate. The second step, clearly time separated, is the deliberate triggering of bilayer formation with the help of poly(ethylene glycol) (PEG), a fusion agent of lipidic vesicles. AFM and FPR measurements confirm that the vesicles do not spontaneously fuse during the first step provided that the streptavidin sublayer is present on the substrate. On the contrary, the treatment with PEG provokes the fast formation of a continuous lipid bilayer, as attested at the hundred nanometer scale by the AFM images and at the hundred micrometer scale by the lateral diffusion of a fluorescent probe ($D = 2.2 \times 10^{-8}$ cm^2 s^{-1} for NBD-DMPE at 22 °C).

Introduction

The reliable and routine formation of supported bilayers mimicking the main properties of biological membranes in biophysics, either as model systems for the fundamental study of biological membranes,[1,2] or for their technological interest,[3−5] is still an experimental challenge. It is important to find a strategy allowing the reconstitution of functional transmembrane proteins in the structure and fully reproducing the lateral mobility of all components of the system.[6] Following the pioneering work on hydrophilic planar surfaces,[7] several experimental variants have been developed on the basis of the spontaneous fusion of vesicles (or proteoliposomes) on surfaces especially modified to organize the interactions between the solid and the bilayer: (i) lipid bilayers simply cushioned on polymer or proteic films,[8−12] (ii) bilayers tethered by hydrophobic molecules anchored to the support via flexible spacers,[5,13−17] and (iii) bilayers tethered via ligand−receptor affinity.[18−21]

The advantages and disadvantages of each variant for the reconstitution of integral membrane proteins were recently carefully discussed.[6] A crucial step is the achievement of spontaneous vesicle fusion on the template, in such a way that a continuous fluid bilayer without defects can be produced in a reasonable time, compatible with the survival of the native membrane proteins.

To overcome the constraints imposed by the uncontrolled kinetics of spontaneous vesicle fusion, we recently proposed a two-step strategy for the assembly of a supported bilayer on a streptavidin sublayer.[22,23] In a first step, intact biotinylated vesicles are accumulated by affinity on the sublayer of immobilized streptavidin. After rinsing, a second step triggers the fast formation of the bilayer by

† Part of the *Langmuir* special issue entitled The Biomolecular Interface.

* Address correspondence to this author at Laboratoire de Technologie Enzymatique, Université de Technologie de Compiègne, B. P. 20529, 60205 Compiègne Cedex, France. Telephone: (33) 3 44 23 44 05. Fax: (33) 3 44 20 39 10. E-mail: Christian.Bourdillon@utc.fr.

‡ Laboratoire de Technologie Enymatique.

§ Laboratoire Roberval.

(1) Brian, A.; McConnell, H. M. *Proc. Natl. Acad. Sci. U.S.A.* **1984**, *81*, 6159−6163.
(2) Lipowsky, R.; Sackmann, E. In *Handbook of Biological Physics*; Elsevier: Amsterdam, 1995; Vol. 1A,B.
(3) Sackmann, E. *Science* **1996**, *271*, 43−48.
(4) Cornell, B. A.; Braach-Maksvytis, V.; King, L. G.; Osman, P. D. J.; Raguse, B.; Wieczoreck, L.; Pace, R. J. *Nature* **1997**, *387*, 580−583.
(5) Stora, T.; Lakey, J. H.; Vogel, H. *Angew. Chem., Int. Ed.* **1999**, *38*, 389−391.
(6) Wagner, M. L.; Tamm, L. K. *Biophys. J.* **2000**, *79*, 1400−1414.
(7) Tamm, L. K.; McConnell, H. M. *Biophys. J.* **1985**, *47*, 105−113.
(8) Kuhner, M.; Tampé, R.; Sackmann, E. *Biophys. J.* **1994**, *67*, 217−226.
(9) Sohling, U.; Schouten, A. J. *Langmuir* **1996**, *12*, 3912−3919.
(10) Feder, T. J.; Weissmuller, G.; Zeks, B.; Sackmann, E. *Phys. Rev. E* **1995**, *51*, 3427−3433.
(11) Wong, J. Y.; Majeswski, J.; Seitz, M.; Park, C. K.; Israelachvili, J. N.; Smith, J. N. *Biophys. J.* **1999**, *77*, 1445−1457.
(12) Wagner, M. L.; Tamm, L. K. *Biophys. J.* **2001**, *81*, 266−275.
(13) Spinke, J.; Yang, J.; Wolf, H.; Liley, M.; Ringsdorf, H.; Knoll, W. *Biophys. J.* **1992**, *63*, 1667−1671.
(14) Naumann, R. A.; Jonczyk, R.; Kopp, J. V.; Esch, H.; Ringsdorf, H.; Knoll, W.; Graber, P. *Angew. Chem., Int. Ed. Engl.* **1995**, *34*, 2056−2058.
(15) Williams, L. M.; Evans, S. D.; Flynn, S. D.; Marsh, A.; Knowles, P. F.; Bushby, R. J.; Boden, N. *Langmuir* **1997**, *13*, 751−757.
(16) Raguse, L.; Braach-Maksvytis, V.; Cornell, B. A.; King, L. G.; Osman, P. D. J.; Pace, R. J.; Wieczoreck., L. *Langmuir* **1998**, *14*, 648−659.
(17) Naumann, C. A.; Prucker, O.; Lehmann, T.; Ruhe, J.; Knoll, W.; Frank, C. W. *Biomacromolecules* **2002**, *3*, 27−35.
(18) Bieri, C.; Ernst, O. P.; Heyse, S.; Hofmann, K. P.; Vogel, H. *Nature Biotechnol.* **1999**, *17*, 1105−1108.
(19) Radler, U.; Marck, J.; Persike, N.; Jung, G.; Tampe, R. *Biophys. J.* **2000**, *79*, 3144−3152.
(20) Stora, T.; Dienes, Z.; Vogel, H.; Duschl, C. *Langmuir* **2000**, *16*, 5471−5478.
(21) Fisher, M. I.; Tjarnhage, T. *Biosens. Bioelectron.* **2000**, *15*, 463−471.
(22) Proux-Delrouyre, V.; Laval, J. M.; Bourdillon, C. *J. Am. Chem. Soc.* **2001**, *123*, 9176−9177.
(23) Proux-Delrouyre, V.; Elie, C.; Laval, J. M.; Moiroux, J.; Bourdillon, C. *Langmuir* **2002**, *18*, 3263−3272.

10.1021/la0260180 CCC: $25.00
Published on Web 10/19/2002

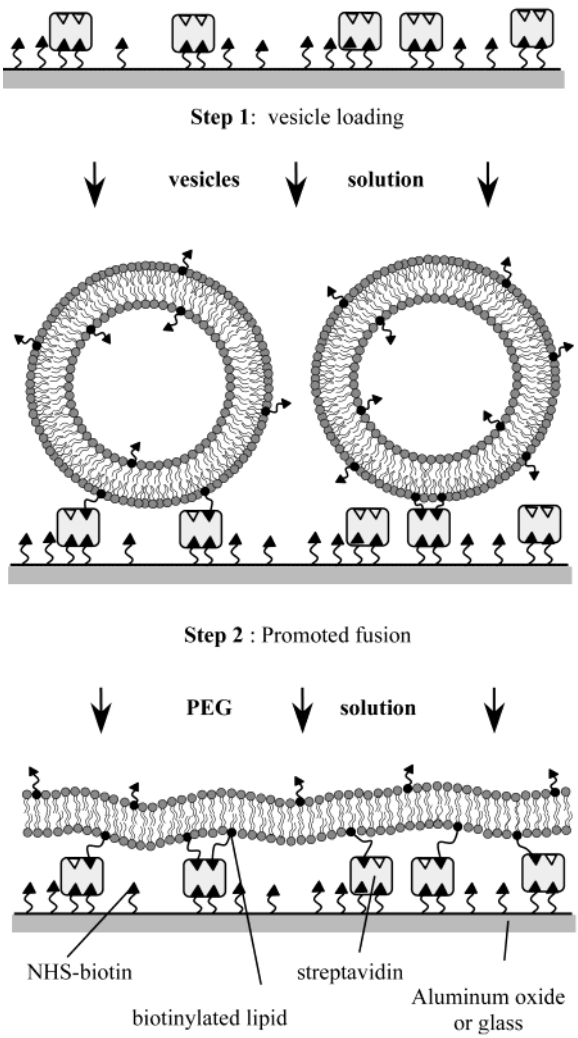

Figure 1. Schematic view of the two-step assembly of streptavidin-supported lipid bilayers on a flat surface of aluminum oxide. Step 1: attachment and accumulation of biotinylated vesicles on a streptavidin layer previously formed on the biotinylated solid interface. Step 2: the vesicle solution is exchanged after rinsing with a PEG solution which induces fusion between the immobilized vesicles. The drawing approximately respects the relative sizes of the components.

addition of poly(ethylene glycol) (PEG), a fusion agent of lipid vesicles (Figure 1). A similar idea was previously proposed to promote vesicle fusion on a polymeric sublayer.[24] The complete loading can be performed in less than 1 h. The efficiency of this strategy was demonstrated first on a honeycomb-like template consisting of aluminum oxide. This special support, referred to as a "microporous electrode", was chosen because it allows one to study the electrochemistry of membrane ubiquinone (Q_{10}), a major electron carrier found in biological electron-transfer chains. The continuity of the final tethered bilayer was ascertained by the electrochemical measurement of both the assembled Q_{10} charge and its lateral mobility.[22]

Despite many advantages, the microporous alumina template cannot be used for most of the bilayer characterizations previously described in the literature, such as microscopy techniques. A primary prerequisite is a flat, nonporous support. We have therefore applied the two-step self-assembly technique to high-quality surfaces. To keep the same chemistry, a thin layer of aluminum, giving spontaneously an alumina surface in air, was vapor-deposited on the glass. Bilayer formation was followed, in particular, to ascertain the efficiency of the PEG treatment, by means of fluorescence microscopy and atomic force microscopy (AFM).

Both techniques are now routinely used for supported bilayer characterization. First, fluorescence microscopy and related techniques such as fluorescence photobleaching recovery (FPR) allow probing of the lateral uniformity and the long-range diffusion properties of the labeled material.[7] In this area, a new element is the recent development of procedures using confocal scanning laser microscopy.[25,26] A complementary technique, atomic force microscopy, has evolved as a routine tool for imaging immobilized biological membranes. It provides better lateral and vertical resolution than optical microscopy, and AFM of lipid membranes offers the advantage of delivering spatially resolved information about material properties such as viscoelasticity, friction, adhesion, and surface charges.[27]

The present study shows that the strategy of deliberate triggering of vesicle fusion is as efficient on flat surfaces as on a microporous template. We demonstrate that (i) the biotinylated vesicles immobilized by affinity on the streptavidin/aluminum oxide surface are stable, (ii) the PEG-triggered fusion is efficiently monitored by fluorescence microscopy and atomic force microscopy, and (iii) the lateral diffusion coefficients of the lipids measured by FPR in the final supported bilayer are consistent with previous reports.

Materials and Methods

Materials. L-α-Dimyristoylphosphatidylcholine (DMPC), L-α-dioleylphosphatidylethanolamine (DOPE), L-α-phosphatidylcholine (egg-PC) type XVI-E from egg yolk, biotin amidocaproic acid 3-sulfo-*N*-hydroxysuccinimide ester (NHS-lc-biotin), octadecyl glucopyranoside (OG), streptavidin, L-α-dipalmitoylphosphatidylethanolamine-*N*-NBD (NBD-DPPE) and poly(ethylene glycol) 8000 (PEG, average molecular weight 8000 g mol^{-1}) were purchased from Sigma (St. Quentin Fallavier, France). 1,2-Dipalmitoyl-*sn*-glycero-3-phosphoethanolamine-*N*-biotinyl (biotinylated DPPE) was from Avanti Polar Lipids (Alabaster, AL). Aminopropyldimethylethoxysilane (ADMS), aminoethanethiol, and octadecyl mercaptan (OM) were from Aldrich (Strasbourg, France). The aluminum rod for vapor deposition (Al 99.95%) was from Merck (Darmstadt, Germany). Organic solvents were HPLC grade. Water with a typical resistivity of 18 MΩ was produced on a Milli-Q purification system (Millipore, Les Ulis, France).

Substrates and Streptavidin Sublayer. Microscope slides (Corning) were first cleaned in chromic acid at 60 °C and thoroughly rinsed in Milli-Q water. They were stored in water until use. Optically transparent aluminum oxide surfaces were made by vapor deposition of a thin layer of aluminum (2 ± 0.1 nm) on the slides (Edwards Model E306A deposition apparatus, working at a pressure below 2×10^{-6} mbar). After the slides had been exposed to air to allow oxide formation, amino groups were created at the aluminum oxide surface by silanization with a freshly prepared ADMS solution in toluene (2% v/v) for 8 h and then thoroughly rinsed with toluene and dried. The streptavidin sublayer was self-assembled on the surface covered with amino groups in two steps. First the slides were dipped for 45 min in a 2 mM NHS-lc-biotin solution in a 50 mM pH 8 phosphate buffer. After thorough rinsing, the slide was dipped for 45 min in a streptavidin solution at a convenient concentration (0.001−0.1 $\mu g\ cm^{-3}$) in PBS buffer (0.01 M, pH 7.4 phosphate buffer + 0.15 M NaCl). After rinsing in a detergent twice (5 min in 50 mM OG),

(24) Seitz, M.; Ter-Ovanesyan, E.; Hausch, M.; Park, C. K.; Zasadzinski, J. A.; Zentel, R.; Israelachvili, J. N. *Langmuir* **2000**, *16*, 6067−6070.

(25) Blonk, J. C. G.; Don, A.; Aalst, H. V.; Birmingham, J. J. *J. Microsc.* **1993**, *169*, 363−374.

(26) Hollars, C. W.; Dunn, R. C. *Biophys. J.* **1998**, *75*, 342−353.

(27) See, for example, a review: Janshoff, A.; Steinem, C. *ChemBioChem* **2001**, *2*, 798−808.

and a last rinsing in the appropriate buffer in at least three different baths, the substrates were ready for experiments aimed at vesicle fusion.

For the blank experiments on glass surfaces (without aluminum) the procedure was identical, as the first step of the assembly (silanization) works as well on glass as on alumina.

Small Unilamellar Vesicles. Lipids, fluorescent probe, and biotinylated DPPE were mixed in the required ratio from stock solutions in chloroform, and then evaporated under nitrogen flow and desiccated under vacuum for 1 h. The dried film was resuspended from the walls of the glass tube by vigorous vortexing in 5 mL of buffer (typically, 1 mM lipids in 0.05 M, pH 7.4 Tris/HNO_3 buffer + 0.1 M $NaNO_3$). Nitrate ions were used instead of the most common chloride ions as we performed the experiments in exactly the same conditions as with microporous electrodes,[23] (chloride severely alters the electrochemical behavior of gold electrodes). This solution was sonicated to clarity, four times for 3 min each, with a Branson Model 250 sonicator (Danbury, CT) set at 60 W, the temperature being maintained at 30 °C. The small unilamellar vesicle (SUV) solution was cleaned of titanium particles by centrifugation at 3000*g* and then diluted at the appropriate concentrations in the Tris buffer.

The size of the vesicles was routinely measured by quasi-elastic light scattering with a Zetasizer 1000/3000 from Malvern Instruments (Malvern, UK). Provided that this measurement was performed less than 2 h after sonication, the average diameter of the SUV was regularly in the 30−50 nm range.

Two-Step Bilayer Formation. In the reference method, the streptavidin sublayer was loaded with the biotinylated vesicles for 1 h in a solution at 0.1 mM in lipids (64.5% egg-PC, 34% DOPE, 0.5% biotinylated DPPE, 1% NBD-DMPE). Extensive rinsing was then performed by exchange of the solutions several times to eliminate the nonspecifically adsorbed vesicles but with care not to allow the air/water meniscus to reach the substrate level.

After the AFM and fluorescence measurements, fusion of the immobilized vesicles was triggered by replacing the buffer solution with a 30% (w/v) PEG solution. After 5 min contact, the concentrated PEG solution was rinsed by gentle stirring with the buffer solution at least 8 times. The tethered bilayers were found to be stable for at least 2 days.

Fluorescence Microscopy and FPR on a Confocal Scanning Light Microscope. A commercial confocal scanning light microscope (CSLM) (LSM 410 from Zeiss, Germany) was used for both fluorescence and fluorescence photobleaching recovery (FPR) measurements. An inverted Zeiss microscope (Axiovert 135) equipped with a 40× oil-immersion objective, NA 1.3 (or for some experiment, a 100× oil-immersion objective, NA 1.3), and with an argon ion laser (488 nm, 15 mW) was controlled by the LSM4 software from Zeiss.

The glass slide was mounted, supported bilayer up, in an open cell allowing the introduction of about 1 mL of solution. The sample cell was placed on the stage of the inverted microscope, and we checked that the thin aluminum layer gave a reasonable attenuation of the light intensity (transmission about 0.5 in the range 450−550 nm).

The uniformity of the emitted fluorescence from the supported bilayer labeled with NBD-DPPE (1−2 mol %) was imaged at 525 nm at a scan speed of 4 s for the production of 512 × 512 pixel images.

The lateral diffusion coefficient of the fluorescent probe was measured by FPR under the following conditions. The scanning mode was used to bleach a square area at full power of the laser. The total scan time used for bleaching was typically 1 s for an area of 45 × 45 μm^2 (with the 40× objective and zoom 8). Occasionally, the bleached area was reduced to 18 × 18 μm^2 and the scan time to 0.5 s (100× objective) for control experiments. Then, the fluorescence recovery of the square together with the surrounding area was regularly imaged at low laser power with a scan time of 4 s (occasionally, 2 s). To avoid as far as possible additional bleaching occurring during the imaging scans, the laser power was attenuated between 800 and 8000 times. For the same reason only a limited series of images was recorded. A sequence of macro commands adapted to the expected characteristic diffusion time was written and run on the CSLM computer for image acquisition. For example, for a bleached square of about 45 × 45 μm^2 and a diffusion coefficient of 2 × 10^{-8} cm^2 s^{-1}, the characteristic diffusion time is 80 s and the following sequence was applied: (i) bleach scan beginning at $t = 0$; (ii) image acquisition beginning at $t = 5$, 25, 45, 65, 85, 105, 185, 285, 385, 485, and 785 s. Quantitative analysis of the gray levels of the images, far from the bleached area, was used to check that the amount of fluorophore bleached during the observation period did not exceed 2% of that bleached initially.

AFM Measurements. A commercial atomic force microscope (Dimension 3100 Nanoscope IIIa, from Digital Instruments) equipped with a tapping-mode liquid cell was employed. The images were recorded under light-tapping conditions with NP-STT20 tips (from Digital instruments, tip radius 20 nm and spring constant 0.12 N m^{-1}), with very low damping (ratio set point of 90%) and at a scan rate between 0.6 and 1.5 Hz. The *z* axis was calibrated by observation of etch pits in muscovite mica substrates. The etch pits were produced by treatment in a concentrated solution of hydrofluoric acid.[28]

The sample slides used for AFM were thermally treated at 430 °C in the course of the vapor deposition of the aluminum layer.[29] This treatment was followed by 1 h of annealing at 450 °C. To minimize contamination of samples and tips, the solutions made with ultrapure water were carefully filtered with 0.2 μm standard filters (Acrodisc) just before use.

Results and Discussion

Formation of Supported Bilayers. In our two-step approach, vesicle immobilization on a streptavidin sublayer was clearly time-separated from PEG-triggered fusion. To allow comparison of the characterization methods, the tethered bilayers were assembled under the same experimental conditions as on our microporous electrodes.[22,23]

The streptavidin sublayer was built layer by layer from the aluminum oxide surface by the following treatments: (i) grafting of aminosilane (ADMS) on the support, (ii) biotinylation of the surface amino group with NHS-lc-biotin, and (iii) docking of streptavidin by exposure to diluted solutions of streptavidin. Small unilamellar vesicles (SUV), biotinylated with 0.5 mol % biotin−DPPE were then accumulated on the sublayer before rinsing. Apart from several blanks, the lipid composition was essentially the same throughout the experiments: 65 mol % egg-PC, 35 mol % DOPE. A small amount of NBD-DPPE (1−2 mol %) was added for the fluorescence measurements.

The lipid composition was chosen for the following reasons. The natural egg-PC mixture does not exhibit a lipid phase transition in the temperature range of the study (20−30 °C) and forms a liquid crystalline phase. In accordance with the literature on vesicle fusion in solution,[30,31] DOPE was introduced to increase the sensitivity of the SUV to PEG fusion.

Confocal Microscopy and FPR Measurements. We used the line-scanning mode of CSLM for both the production of the bleached area at full laser power and the imaging of the fluorescence recovery as a function of time at low excitation energy. Specific methodologies and theories have been developed for FPR experiments on confocal microscopes (i.e., line scanning microphotolysis),[32,33] but here neither a very small photobleached area nor a fast temporal resolution was needed, as large surface

(28) Nagahara, L. A.; Hashimoto, K.; Fujishima, A.; Snowden-Ifft, D.; Price, P. B. *J. Vac. Sci. Technol.* **1994**, *12*, 1694−1697.
(29) Liu, Z. H.; Brown, N. M. D. *Thin Solid Films* **1997**, *300*, 84−94.
(30) Yamazaki, M.; Ito, T. *Biochemistry* **1990**, *29*, 1309−1314.
(31) Lee, J.; Lentz, B. R. *Proc. Natl. Acad. Sci. U.S.A.* **1998**, *95*, 9274−9279.
(32) Kubitscheck, U.; Wedekind, P.; Peters, R. *Biophys. J.* **1994**, *67*, 948−956.
(33) Wedekind, P.; Kubitscheck, U.; Heinrich, O.; Peters, R. *Biophys. J.* **1996**, *71*, 1621−1632.

areas (hundred of micrometers) of continuous flat bilayers were available. These low constraints on both time and space allowed us to use the theoretical framework originally proposed by Axelrod et al. for conventional FPR.[34,35]

The fluorescent probe initially distributed uniformly in an infinite, flat membrane produced an image with an initial intensity noted $F(i)$. Rapid scanning at full laser power on a small area of the membrane (about 18×18 μm^2 or 45×45 μm^2) led to a uniform fluorescence intensity inside the bleached area, $F(0)$. The recovery images, exhibiting fluorescent level vs time $F(t)$ in the bleached area, contain the information needed to analyze the transport process. For freely diffusing molecules, complete fluorescence recovery occurs for infinite time at a $F(\infty) = F(i)$ level corresponding to a mobile fraction of 100%. The mobile fraction as a percentage is defined as

$$M = 100[F(\infty) - F(0)]/[F(i) - F(0)] \quad (1)$$

The data are more conveniently displayed in the form of fractional fluorescence recovery curves $f(t)$ defined as[34]

$$f(t) = [F(t) - F(0)]/[F(i) - F(0)] \quad (2)$$

Taking into account the high lateral resolution of the beam in CSLM and the relative large size of the area bleached, the scanning mode allowed the production of a bleached area corresponding to the theoretical conditions referred to as the "uniform circle profile" in Axelrod's paper (the only difference here is the shape of the spot, which is a square and not a disk).

With the hypothesis of a pure two-dimensional diffusion of the fluorescent probe from an infinite reservoir, the fractional fluorescence recovery as a function of time t is then given by[35]

$$f(t) = \exp(-2\tau_D/t)[I_0(2\tau_D/t) - I_1(2\tau_D/t)] \quad (3)$$

I_0 and I_1 are modified Bessel functions, $\tau_D = w^2/4D$ is the characteristic diffusion time, and w is the radius of the bleached area at $t = 0$. To take into account the slight geometrical difference (the square imposed by the mechanical scanning), w is here defined by a disk of equivalent area; $w = (A/\pi)^{0.5}$ where A is the area of the bleached square and thus $\tau_D = A/4\pi D$. The experimental values of A were carefully calibrated on CSLM images produced in nondiffusive conditions. We have checked that the experimental conditions satisfied the hypothesis related to the diffusion law:

(i) The area of the supported bilayer (several mm^2 on the slide surface) was at least 100 times the bleached area (infinite reservoir hypothesis).

(ii) The bleaching times (0.5 s for 18×18 μm^2 and 1 s for 45×45 μm^2) were negligible compared to the characteristic diffusion times (less than 5% of τ_D as recommended).[34] For example, for a diffusion coefficient of 2×10^{-8} cm^2 s^{-1} the characteristic time was 80 s when the bleached area was 45×45 μm^2.

(iii) As the rate of image acquisition is not very high on the CSLM (typically, 4 s for a convenient signal-to-noise ratio), we chose to extrapolate the $F(0)$ value at $t = 0$ from the first three or four recorded fluorescence intensities $F(t)$ plotted as a function of the square root of time.

The lateral diffusion coefficients were evaluated from the best fit between the recovery curves calculated from eq 3 and the experimental data. Figure 2 shows typical recovery data obtained for a mobile fluorophore. This serves also a reference blank because this experiment was performed on a solid-supported bilayer directly fused on a clean glass surface according to the McConnell protocol.[1] The mobile fraction ($100\% \pm 5\%$) and the lateral diffusion coefficient found for the NBD-DPPE probe ($D = 2.1 \times 10^{-8} \pm 0.4 \times 10^{-8}$ cm^2 s^{-1} at 22 °C, average value on three series of glass surfaces) are in accordance with previous literature results (D from 1.5×10^{-8} to 2.5×10^{-8} cm^2 s^{-1} at ambient temperature and from 4×10^{-8} to 5×10^{-8} cm^2 s^{-1} at 30 °C).[7,12,36,37] We also checked that D, the "long-range" diffusion coefficient, was independent of the size of the bleached area (from 18×18 μm^2 to 45×45 μm^2).

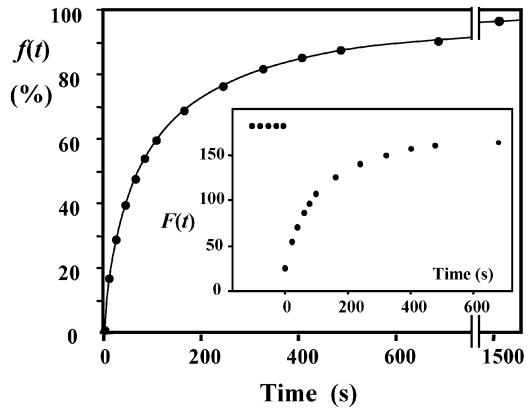

Figure 2. Typical fractional fluorescence recovery curve of the fluorescent probe (NBD-DMPE, 2 mol %) in mixed egg-PC−DOPE bilayer obtained after spontaneous vesicle fusion on glass surfaces according to the protocol of McConnell (SUV 1 mM in Tris buffer).[1] The experimental data (●) calculated from eq 2 were fitted by eq 3. The curve was computed with the following constants: $D = 2.2 \times 10^{-8}$ cm^2 s^{-1}, $A = 2.07 \times 10^{-5}$ cm^2, and $M = 100\%$. Temperature 22 °C. The insert shows the raw fluorescence intensity ($F(t)$, in relative units) integrated on the bleached area of the CSLM images. Bleaching time = 1 s. Time sequence as in Material and Methods.

The primary goal of the fluorescence experiments was to study the efficiency of PEG treatment on vesicle fusion. We therefore evaluated the lateral dynamic properties of the lipids before and after this treatment. The main result on our alumina surface is presented in Figure 3. Before PEG treatment, the absence of recovery in the sequence of fluorescence images (Figure 3A) demonstrates both that the vesicles are correctly immobilized on the streptavidin sublayer and that the long-range fusion is negligible ($D = 10^{-11}$ cm^2 s^{-1}). The result is similar to the lack of vesicle fusion electrochemically detected in the same kind of experiment previously performed on microporous electrodes.[22,23] After PEG treatment (Figure 3B), the behavior of the bleached area is completely different. The lateral diffusion of the NBD-DPPE probe was proved by the recovery in the bleached area, with a mobile fraction close to 100% and a diffusion coefficient of 2×10^{-8} cm^2 s^{-1}. As already found in the experiments on the microporous structure,[22,23] the short exposure of the immobilized vesicles to the fusogen agent provokes the formation of a continuous bilayer on the streptavidin support, as shown schematically in Figure 1.

One potential advantage of this two-step strategy is related to the fact that the fusion can be triggered at a chosen time. Evidently, this is possible only if vesicle fusion does not occur spontaneously before PEG promotion. We

(34) Axelrod, D.; Koppel, D. E.; Schlessinger, J.; Elson, E.; Webb, W. W. *Biophys. J.* **1976**, *16*, 1055−1069.
(35) Soumpasis, D. M. *Biophys. J.* **1983**, *41*, 95−97.
(36) Schmidt, T.; Schutz, G. J.; Baumgartner, W.; Gruber, H. J.; Schindler, H. *Proc. Natl. Acad. Sci. U.S.A.* **1996**, *93*, 2926−2929.
(37) Tocanne, J. F.; Dupou-Cezanne, L.; Lopez, A. *Prog. Lipid Res.* **1994**, *33*, 203−207.

Table 1. Consequence of the PEG Treatment on the Formation and Lateral Dynamics of Supported or Tethered Bilayers on Various Surfaces[a]

substrate	silanization and biotinylation	streptavidin	vesicle solution for loading C	lateral diffusion coeff, D (cm^2 s^{-1}) (mobile fraction, M (%))	
				before PEG	after PEG
glass	no	no	egg-PC 1 mM	$2.0 \times 10^{-8} \pm 0.6 \times 10^{-8}$ (100 ± 5%)	2×10^{-8} (100%)
glass	no	no	egg-PC + DOPE 0.1 mM	$2.1 \times 10^{-8} \pm 0.6 \times 10^{-8}$ (100 ± 5%)	2×10^{-8} (100%)
glass	yes	yes 0.01 μg/mL	biotinylated egg-PC + DOPE 0.1 mM	$<10^{-11}$	$1.9 \times 10^{-8} \pm 0.6 \times 10^{-8}$ (100 ± 5%)
aluminum oxide	no	no	egg-PC + DOPE 0.01−1 mM	$<10^{-11}$ low fluorescence at C < 0.1 mM)	2.5×10^{-8} irreproducible at C < 0.1 mM
aluminum oxide	yes	yes 0.01−0.1 μg/mL	biotinylated egg-PC + DOPE 0.1 mM	$<10^{-11}$	$2.2 \times 10^{-8} \pm 0.6 \times 10^{-8}$ (95 ± 5%)
aluminum oxide	yes	yes 0.01 μg/mL	egg-PC + DOPE 0.01−1 mM no biotin	$<10^{-11}$ low fluorescence at C < 0.1 mM	2×10^{-8} irreproducible at C < 0.1 mM

[a] After PEG means 5 min in a 30% (w/v) PEG-8000 solution in the buffer and thorough rinsing. Mobile fraction and lateral diffusion coefficient of NBD-DMPE measured by FPR at 21−22 °C.

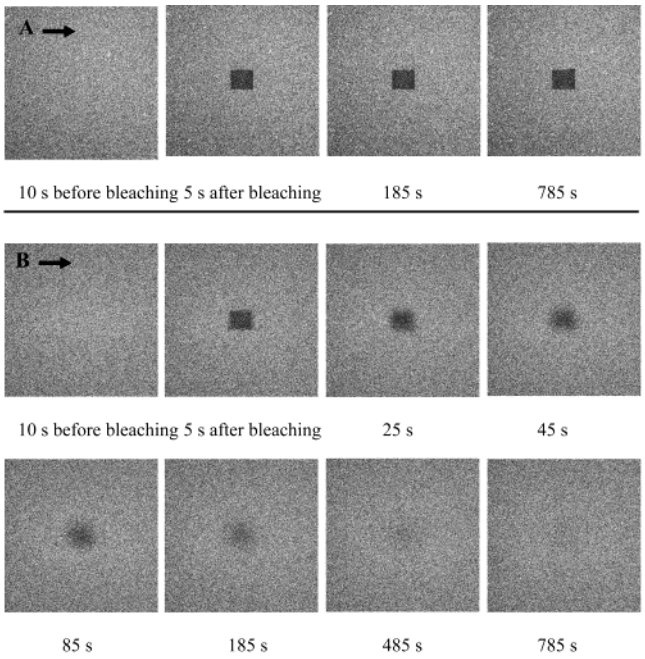

Figure 3. Fluorescence photobleaching experiments demonstrating the efficiency of PEG treatment on the formation of the continuous lipid bilayer. Images: 310 × 310 μm; bleached spot: 49 × 42 μm. (A) Sequences of scanning confocal images recorded before PEG treatment of the alumina/streptavidin surface loaded with biotinylated vesicles (the reference method is described in Material and Methods). (B) The same FPR experiment after PEG treatment. Interpretation of the fluorescence recovery data such as in Figure 2 gives $D = 1.9 \times 10^{-8}$ cm^2 s^{-1}, $A = 2.07 \times 10^{-5}$ cm^2, and $M = 95\%$. Temperature 21 °C. The fluorescent probe was NBD-DPPE at 2 mol %.

studied the effects of the support and of the sublayers on adsorption and spontaneous fusion. It is already known that a (cleaned) bare glass surface promotes SUV fusion[1] and, on the contrary, that an aluminum oxide surface can be used as a barrier between supported bilayers.[38] The FPR results presented in Table 1 reproduce these behaviors. On glass, SUV of pure egg-PC or of mixed egg-PC/DMPE lipids fuse spontaneously and the PEG treatment induces no additional modification of the lateral lipid mobility. On bare aluminum oxide, the SUV are adsorbed (clearly at the relatively high lipid concentration of 1 mM) (line 4 of the table) but the fluorescent probe is immobile. After PEG treatment fusion occurs, as attested by the lateral mobility of the probe, but this experiment appears to be reproducible only when the lipid concentration in SUV solution is higher than 0.1 mM. At lower lipid concentrations, the lack of fluorescence recovery indicates the presence of too small an amount of adsorbed material for the formation of a continuous bilayer.

If now both the glass and aluminum oxide surfaces are modified by successive aminosilane, NHS-biotin, and streptavidin loading, and if the modified surfaces are incubated with biotinylated vesicles (lines 3 and 5), no lateral mobility is observed ($D < 10^{-11}$ cm^2 s^{-1}) before PEG treatment. However, the surfaces are covered, as expected, with immobilized vesicles as attested at this scale by a uniform fluorescence (as in Figure 3A, for example). PEG treatment performed after rinsing the SUV solution induces fusion of the immobilized material on both surfaces (identical mobility of about 2×10^{-8} cm^2 s^{-1}). These results on glass and aluminum oxide are consistent with the following conclusions:

(i) A streptavidin sublayer is convenient for the immobilization of intact biotinylated vesicles. This confirms previous reports.[39,40]

(ii) The streptavidin sublayer inhibits spontaneous vesicle fusion which occurs classically on bare glass surfaces.

(iii) The mechanism of the triggered fusion by PEG does not depend on the substrate supporting the streptavidin sublayer.

Finally, the behavior described above for bare aluminum oxide was reproduced on the streptavidin sublayer when biotin−DPPE was omitted from the vesicles. These last control experiments are summarized on line 6 (Table 1). The lack of affinity between vesicles and the sublayer leads to a failure in the bilayer continuity only at very low lipid concentrations. This is not a surprising result as it is known that any surface adsorbs amphiphilic molecules. A PEG treatment on this adsorbed material can provoke bilayer formation, but in this case, even if the bilayer appears fluid and continuous, it is not tethered on the streptavidin sublayer and the structure is clearly less controlled.

(38) Groves, J. T.; Ulman, N.; Cremer, P. S.; Boxer, S. G. *Langmuir* **1998**, *14*, 3347−3350.

(39) Kroger, D.; Hucho, F.; Vogel, H. *Anal. Chem*. **1999**, *71*, 3157−3165.

(40) Percot, X.; Zhu, X.; Lafleur, M. *Bioconjugate Chem*. **2000**, *11*, 674−678.

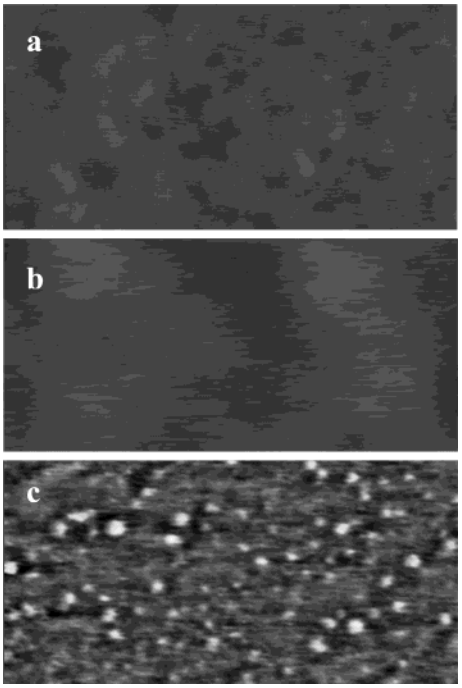

Figure 4. AFM topographic images at the same scale (500 nm × 250 nm, *z* scale 15 nm) of aluminum oxide surface at different steps of the assembly of the streptavidin sublayer. (a) Bare surface; (b) after silanization and NHS-biotin treatment; (c) after streptavidin loading for 45 min in a solution at 1 ng cm^{-3} and rinsing. Scans in Tris buffer solution at 0.6 Hz, at very low damping (ratio set point 90%).

Tapping-Mode Atomic Force Microscopy. The aim is to follow again, but here at the nanometer scale, the step-by-step assembly of the supported bilayer structure and particularly the fusion of the vesicles. All the AFM experiments were performed in a liquid cell immersed in buffer solution (0.05 M, pH 7.4 Tris/HNO_3 buffer + 0.1 M $NaNO_3$).

The first point was to produce highly flat surfaces of aluminum oxide. We used glass slides as templates heated at 430 °C during the vacuum vapor deposition of about 10 nm of aluminum (deposition rate < 0.1 nm s^{-1}). The samples were then annealed for 1 h at 450 °C in air.[29] Observation of the surface revealed convenient flat areas of about 3 × 3 μm, close to atomically flat surfaces (root-mean-square (rms) roughness of 0.2 nm, Figure 4a) separated by uncontrolled protuberant structures.

Silanization of the oxide surface with a short-chain aminosilane changed only slightly the roughness (0.3 nm instead of 0.2 nm), and the image was essentially identical (not shown). On the contrary, NHS-biotin is a larger flexible molecule about 2.3 nm long.[41] After the biotinylation treatment, the rms roughness increased to 0.6 nm, demonstrating the grafting of a new layer (Figure 4b), but the biotin moiety itself is a too small to be clearly observed with this technique.

The next step was the optimization of the protein surface concentration in the streptavidin sublayer. As biotin is considerably smaller than streptavidin (the tetramer molecule is often described as a rough ca. 5 nm cube),[42] we assumed that the biotin surface concentration in the immobilized layer is in a large potential excess. Taking into account the high affinity between biotin and streptavidin, the simplest way to modulate the streptavidin surface concentration is to load the surface under diffusion-limited conditions. The biotinylated surfaces were therefore incubated for a constant time (45 min) in solutions of streptavidin at very low concentration. The useful concentration range under these experimental conditions was found to be between 10^{-10} and 10^{-12} mol L^{-1} streptavidin. At the middle of this concentration range (typically 1 ng cm^{-3}), the immobilized streptavidin molecules appear to be regularly dispersed on the surface (Figures 4c and 5a). The measured size of the individual streptavidin (2 nm high and 18 nm in diameter) does not exactly match with the 5 × 5 × 5 nm cube model.[42] The too-large apparent diameter can easily be explained by the phenomenon known as dilatation,[43,44] taking into account that the tip curvature radius was here 20 nm. The difference in height can be explained by the fact that neither the layer under the streptavidin molecule nor the streptavidin molecule is rigid. According to recent tapping-mode AFM studies on soft materials such as methacrylate copolymers,[45] the apparent profile could be the result of two contributions: the true height difference and the difference in the local mechanical properties of the protein and the underlayer.

Under the loading conditions of Figure 4c, the density of the streptavidin molecules can be evaluated at about $(9 \pm 4) \times 10^{10}$ molecules per cm^2 of aluminum oxide surface (1.5×10^{-13} mol cm^{-2}, average on four samples). The average distance between adjacent molecules is therefore 25−30 nm. If we use the 5 × 5 × 5 nm cube model, the surface concentration of a monolayer of close packed streptavidin molecules is estimated to be about 4×10^{12} molecules per cm^2 (6.7×10^{-12} mol cm^{-2}). The surface ratio of the oxide surface covered with streptavidin was then 2% under the experimental conditions.

When the streptavidin concentration was increased to 10 ng cm^{-3} or more, the surface coverage increased, but the surface is polluted by many streptavidin aggregates (not shown). On the contrary, for very low 1.7×10^{-12} mol L^{-1} concentration (0.1 ng cm^{-3}), the coverage is inhomogeneous and the density of less than 10^{10} molecule per cm^2 is too low. Further experiments were performed with the experimental conditions of Figure 4c.

The final stage of bilayer formation is the loading of the lipidic material according to our two-step procedure. Figure 5b shows the immobilization of the biotinylated vesicles on the streptavidin paving of Figure 5a. Adsorbed intact vesicles have already been observed by AFM, in general under solution.[46−48] In our case, the topology indicates structures whose diameters vary between 30 and 110 nm and heights between 10 and 20 nm. Measurement of the average vesicle size by light scattering on the same vesicle solution gave an average diameter of 58 nm, i.e., in a similar range. However, AFM indicates that the heights of the immobilized vesicles are systematically smaller than expected compared to the apparent topographic diameter. The dilatation effect alone cannot explain this result, as the tip diameter is here smaller than the vesicles. Apparently, the immobilized vesicles are distorted into oblate disks by interaction with the

(41) In *Bioconjugate Techniques*; Hermanson, G. T., Ed.; Academic Press: New York, 1996; pp 371−400.
(42) See, for example: Darst, S. A.; Ahlers, M.; Meller, P. H.; Kubalek; E. W.; Blakenbourg, R.; Ribi, H. O.; Ringsdorf, H.; Kornberg, R. D. *Biophys. J.* **1991**, *59*, 387−396.
(43) Keller, D. J.; Franke, F. S. *Surf. Sci.* **1993**, *294*, 409−419.
(44) Markiewiecz, P.; Goh, M. C. *Langmuir* **1994**, *10*, 5−7.
(45) Kopp-Marsadon, S.; Leclère, P.; Dubourg, F. Lazzaroni, R.; Aimé, J. P. *Langmuir* **2000**, *16*, 8434−8437.
(46) Singh, S.; Keller, D. J. *Biophys. J.* **1991**, *60*, 1404−1410.
(47) Reviakine, I.; Brisson, A. *Langmuir* **2000**, *16*, 1806−1815.
(48) Leonenko, Z. K.; Carmini, A.; Cramb, D. T. *Biochim. Biophys. Acta, Biomembranes* **2000**, *1509*, 131−147.

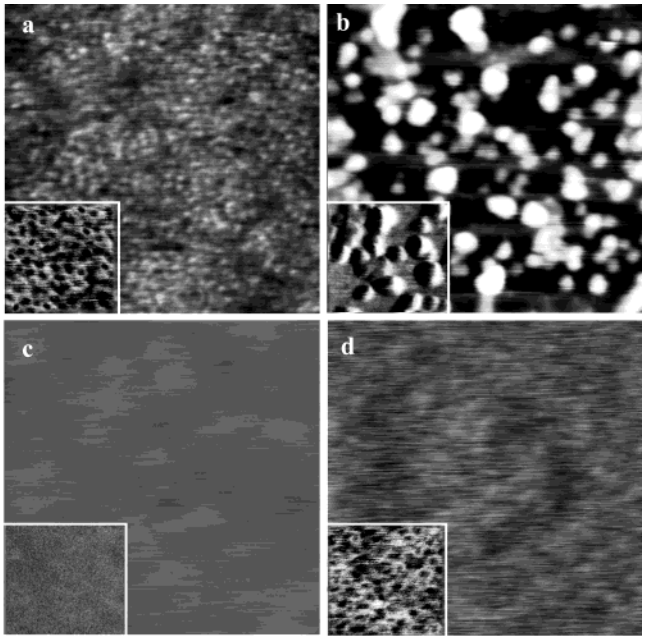

Figure 5. AFM topographic images (1 μm × 1 μm, *z* scale 30 nm) and phase images (inset at the same scale in the bottom left corner) of the aluminum oxide surface at different steps of the supported lipid bilayer assembly (four images not exactly at the same place of the same sample). (a) The streptavidin sublayer at lower magnification than Figure 4c and showing the regular protein paving. (b) Vesicles immobilized on the streptavidin sublayer (loading of biotinylated mixed egg-PC−DOPE vesicles at a concentration of 0.1 mM for 1 h and rinsing). (c) The result of PEG treatment of the immobilized vesicles (5 min in PEG-8000 30% m/w). A suspended and continuous bilayer covers the streptavidin sublayer. (d) Control: the supported bilayer was eliminated with a strong detergent (OG 50 mM) and the detergent thoroughly washed off.

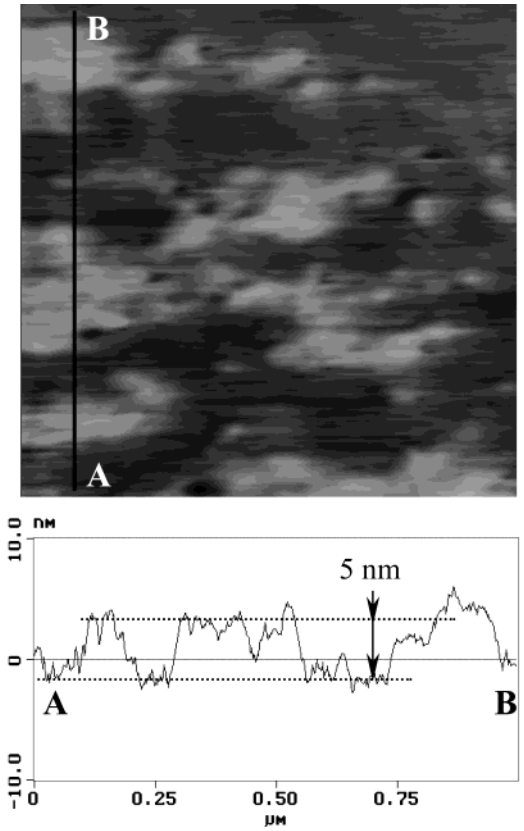

Figure 6. AFM topographic image (1 μm × 1 μm, *z* scale 30 nm) after PEG treatment in the case of a low density of immobilized vesicles (loading of biotinylated vesicles at a concentration of 10 μM for 1 h and rinsing). The cross section (line A−B) shows partial lipidic bilayer domains about 5 nm thick.

support. A similar situation has already been described for vesicles adsorbed on mica.[48]

We checked that the vesicles were firmly immobilized by scanning the same area every 6 h. Provided that the small drift of the piezoactuator is corrected, the vesicles stay in the same place and the vesicle density is unchanged after 24 h.

Under the loading conditions of Figure 5b, the immobilized vesicle density was estimated to be 1.2×10^{10} vesicles cm^{-2}. As the fusion treatment was applied in the absence of free vesicles in solution, the question is whether such an amount of immobilized lipidic material is sufficient to produce the expected continuous bilayer. Let us calculate approximately the minimum vesicle density needed for the formation after fusion of a continuous unilamellar bilayer. The surface concentration in a monolayer of lipid is about 2.5×10^{-12} mol cm^{-2} (60−65 Å^2 per phospholipid molecule),[1,49] thus 5×10^{-10} mol cm^{-2} for a bilayer. A vesicle 60 nm in diameter represents about 3.4×10^4 phospholipid molecules. The minimal vesicle density is then $5 \times 10^{-10}(N/3.4 \times 10^4) = 8.8 \times 10^9$ vesicles cm^{-2}. The density measured in Figure 5b is approximately 30% in excess. Under these conditions PEG-triggered fusion of the immobilized vesicles leads to a continuous bilayer, as validated by the very flat topography of Figure 5c. In several similar experiments, the apparent typical rms roughness was about 0.2 nm and the observed surfaces were clearly more flat than the streptavidin sublayer. Despite the low density of the streptavidin "pillars" (about 2% of the surface area) the tethered bilayer seems able to isolate mechanically the support at the tip frequency used.

On the contrary, the bilayer cannot cover the entire surface if the amount of immobilized lipidic material is too low, as for example at the low lipidic concentration of 10 μM (Figure 6). However, PEG-promoted formation of the supported bilayer begins under these conditions, as indicated by the apparent thickness (about 5 nm) of the partial bilayer domains found on the cross section shown in Figure 6. In the literature, this partial coverage has often been observed by AFM in the course of the kinetics of spontaneous vesicle fusion and coalescence between planar lipid domains on glass or mica.[46,47]

A last check was performed after removal of the tethered bilayer by means of a concentrated detergent (50 mM OG). In this situation only a few biotinylated DPPE molecules embedded in the streptavidin sublayer remain in place after the destruction of the bilayer. The streptavidin paving was imaged again after thorough rinsing of the detergent (Figure 5d). The lesser quality of the topographic image (compared to Figure 5a) is doubtless the result of tip contamination with the detergent. Apparently, the phase images are less sensitive to this contamination, as the streptavidin paving appears to be similar on the phase inlays of Figure 5a,c.

Conclusion

We demonstrate here that supported and tethered lipid bilayers can easily be produced by a time-separated two-step procedure which consists of the accumulation of intact vesicles followed by deliberate triggered fusion.

(49) Nollert, P.; Kiefer, H.; Jahning, F. *Biophys. J.* **1995**, *69*, 1447−1455.

First, the immobilization of intact vesicles on a streptavidin sublayer was ascertained by microscopy. Measurements with fluorescence microscopy and the related FPR technique show that the fluorescent probe present in the vesicles is immobile at the hundred micrometer scale. Similarly, direct observation of the vesicles at the hundred nanometer scale by tapping-mode AFM demonstrates that they are firmly immobilized on the sublayer. This situation without fusion can be maintained for hours.

Second, the introduction of a powerful fusogen agent, such as a solution of PEG, promotes the formation of a continuous and uniform bilayer, without defects at the two scales observed. The lateral mobility of the fluorescent probe is found to have the expected value $D = 2 \times 10^{-8}$ cm^2 s^{-1} at 21 °C by FPR, and the AFM images show a continuous and remarkably flat, smooth bilayer surface. These results produced on plane surfaces of glass and aluminum oxide confirm and extend the previous measurements performed by electrochemical methods on the aluminum oxide microporous template.[22,23]

Compared to the numerous strategies of "spontaneous" vesicle fusion found in the literature, these results suggest that a strategy including a step of triggered fusion opens new possibilities. For example, the formation and the properties of the tethered bilayers are found to be identical whatever the template (glass or aluminum oxide) of the streptavidin sublayer. This demonstrates that the nature of the substrate can be dissimulated in the course of streptavidin immobilization and opens up the possibility of rational and broader choices for the substrate. One limitation is the need for phosphatidylethanolamine (PE) heads in the lipid mixture, as PE was found essential in the PEG-promoted fusion.[50] However, PE polar groups are very common in natural membranes (often at a percentage higher than 20%) and this constraint would not alter the potentialities of the method for the introduction of membrane proteins in such biomimetic structures.

Note Added after ASAP Posting. This article was released ASAP on 10/19/2002 with an error in the acronym for dipalmitoylphosphatidylethanolamine. The correct version was posted on 01/17/2003.

Acknowledgment. We thank Nicolas Carreau and Thierry Thomasset for help with the macro language of the scanning confocal microscope. This work was partially supported by a research grant from ANVAR.

LA0260180

(50) Haque, M. E.; McIntosh, T. J.; Lentz, B. R. *Biochemistry* **2001**, *40*, 4340−4348.